

Convective self-assembly to deposit supported ultra-thin mesoporous silica films

Zhen Yuan,^a D. Bruce Burckel,^b Plamen Atanassov*^a and Hongyou Fan*^{ab}

Received 22nd August 2006, Accepted 9th October 2006

First published as an Advance Article on the web 20th October 2006

DOI: 10.1039/b612091a

For practical consideration in applying mesoporous films for sensors, it is ideal to fabricate thinner films to achieve fast transport and therefore rapid response. Here we report a new, facile method to deposit mesoporous silica films with thickness less than 100 nm through combining convective self-assembly and surfactant/silica self-assembly. Through an interfacial capillarity defined in the wedge between two substrates, a meniscus of solutions containing silicate, surfactant, alcohol, and water is formed. While the solvent evaporates during the film formation, the solution from the bulk droplet spreads to the drying region, enriching the surfactant/silica concentration at the edge of the meniscus by the convective flux of solvent. The continuous evaporation, spreading, and enriching induce surfactant and silica self-assembly in the bulk droplet to form an ordered surfactant/silica liquid crystal mesophase film. After calcination, supported ultra-thin films are formed containing interconnected mesopore channels with high surface areas. The combined self-assembly process relies on the evaporation of the solvents to form ordered mesostructures, which enables the deposition of patterned films and ultimately makes this combined technique ideal for device fabrication.

Introduction

Surfactant templated mesoporous thin films could find wide applications in membrane-based separation, selective catalysis and sensors.¹ Recently, mesoporous silica films have been demonstrated for electronic and optical applications,^{2,3} such as low-*k* dielectric materials for integrated circuits.² Since the invention of surfactant templating techniques, several approaches have been developed to make mesoporous thin films. Yang *et al.*⁴ reported a hydrothermal self-assembly process to deposit mesostructured silica/surfactant composite films on a mica surface. Subsequent calcination at high temperature (>400 °C) in air led to mesoporous silica films that exhibit 1-dimensional (1-D) hexagonal mesostructure with pore channels parallel to the substrates. Later a similar process was applied to synthesize mesoporous films on graphite.⁵ Combining self-assembly and conventional sol-gel chemistry, Brinker *et al.*⁶ developed an evaporation-induced self-assembly (EISA) process to deposit mesoporous films on solid substrates through dip- or spin-coating. The resulting films exhibited lamellar, 2-D hexagonal, 3-D hexagonal or cubic mesostructures. EISA has been extended to deposit multifunctional films and those with patterned features through micro-pen and ink-jet printing lithographic process⁷ as well as films deposited through an aerosol-EISA process.⁸ Recently, Nishiyama *et al.*^{9–11} reported a vapor phase approach to synthesize mesoporous silica films. A pure surfactant film was

deposited on the substrate first. Subsequently the surfactant film was placed in an autoclave reactor containing silicate precursor and hydrochloric acid aqueous solutions. Mesoporous silica films were obtained after several hours at hydrothermal conditions, followed by calcination. For practical consideration in applying mesoporous films for sensors, it is ideal to fabricate thinner films to achieve fast transport and therefore rapid response. In this work, we report a simple method to deposit ultra-thin (<100 nm) mesoporous silica films by combining convective and surfactant/silica self-assembly.¹² This is the first report in which such a technique is applied to templated mesostructured metal oxide films.

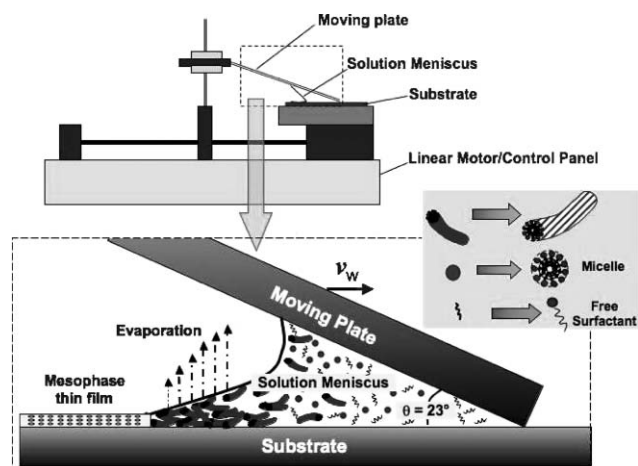
The method of “convective assembly” or “convective self-assembly” was developed originally for controlled deposition of micro- and nanoparticle coatings by Denkov *et al.*,^{13,14} and further modified for a more scalable device by Prevo and Velev.¹⁵ It has been defined as the mechanism of self-assembly of colloidal particle suspensions in thin evaporating films: the flow of water caused by solvent evaporation leads the particles or subject to self-assemble onto a substrate in an ordered way. Using convective assembly, it is possible to generate large scale, highly ordered films on the substrate.¹⁶ This process is driven by balanced volumetric flux of solvent evaporation and particle assembly. According to Dimitrov and Nagayama¹⁷ and Prevo and Velev,¹⁵ the film deposition kinetics are given by:

$$v_c = \frac{K\phi}{h(1-\varepsilon)(1-\phi)} \approx \frac{K\phi}{h(1-\varepsilon)}, \text{ for } \phi \ll 1 \quad (1)$$

where v_c is the film formation velocity, v_w is the coating plate moving speed (see Scheme 1), h is the film thickness; ε is the porosity of the deposited colloidal films, which can be

^aThe University of New Mexico/NSF Center for Micro-Engineered Materials, Department of Chemical and Nuclear Engineering, Albuquerque, NM, 87131, USA. E-mail: plamen@unm.edu; hfan@sandia.gov

^bCeramic Processing and Inorganic Materials Department, Sandia National Laboratories, Albuquerque, NM, 87106, USA



Scheme 1 Illustration of the formation of a silica/surfactant thin film mesophase on a solid substrate by combined convective and surfactant self-assembly. An aliquot of 5–10 μl surfactant–silica sol solution (see Experimental for solution preparation) was placed at the junction of two microscopy slides or silicon wafers held at an angle of $23 \pm 1^\circ$ to form a meniscus along the line of contact. The electric linear motor pushes the moving plate (droplet plate) and drags the solution across the substrate at a constant velocity in the range from 80 to 230 $\mu\text{m s}^{-1}$ at ambient conditions with a controlled humidity of $\sim 30\%$ RH. The films were formed and dried on the substrate as the solvent evaporated.

quantitatively defined as the ratio of pore volume to the total volume of materials in the case of porous film. ϕ is the volume fraction of the particles in suspension; here it refers to the volume fraction of the surfactant in suspension. K is a hydrodynamic parameter which accounts for the convective contribution to the molecular transport. For the mesoporous film formation described below, v_c represents the certain velocity for formation of a complete and uniform film of a particular film thickness; and v_w is defined as in eqn (1), which is the coating plate moving speed. When the deposition speed was equal to the film formation for a certain film thickness, $v_c = v_w$. In the case of mesoporous silica film formation, ϕ and K can be combined as another constant κ under conditions of constant temperature and humidity, under which condition the evaporation of the solvent keeps constant. That simplifies the relationship between coating velocity and film thickness to a linear correlation. By varying the velocity and film thickness, $\kappa = (K\phi)$ can be determined.

Experimental

All chemicals were obtained from Aldrich and used without further purification unless noted elsewhere.

Preparation of coating solution

The silica–surfactant solution was prepared using a formula designed to minimize the siloxane condensation rate. A two-step acid catalyzed hydrolysis and condensation reaction was used to prepare the silica sols.

(1) Preparation of silica sols: tetraethyl orthosilicate (TEOS), ethanol, de-ionized water, and 0.07 N HCl were mixed in a Pyrex reaction kettle in the molar ratio (TEOS) 1.0 : (EtOH) 3.8 : (H_2O) 1.1 : (HCl) 5×10^{-5} and refluxed at 60 $^\circ\text{C}$ for

90 min. The resulting solution was cooled to room temperature and stored at -20°C .

(2) Preparation of silicate sol with surfactants: normally, the above silicate sol was diluted with ethanol (volume ratio 1 : 2) followed by addition of water and dilute HCl (0.07 N) aqueous solution. Surfactants were added in the amounts needed to achieve initial surfactant concentrations c_0 ranging from 0.004 to 0.23 M. The final molar ratio is 1 TEOS : 22 $\text{C}_2\text{H}_5\text{OH}$: 5 H_2O : 0.004 HCl : 0.02–0.2 surfactant. The surfactants were removed by calcination in air at 450 $^\circ\text{C}$ for 3 h (heating rate 1 $^\circ\text{C min}^{-1}$). Coatings were deposited on polished (100)-silicon or glass slides with velocities ranging from 80 to 230 $\mu\text{m s}^{-1}$. The substrates, silicon wafer chips were cleaned by immersion in a piranha solution (30% H_2O_2 : 96%–98% $\text{H}_2\text{SO}_4 = 1 : 3$. **CAUTION:** dangerous and aggressive solution) for an hour, then in 1 N NaOH for 10–15 min. Then the Si wafers were rinsed with deionized (DI) water thoroughly and dried by pure nitrogen gas.

Preparation of patterned films

Cleaned (100)-silicon wafers were spin-coated with commercial i-Line photo-resist (NR7-500PY, Futurrex), and patterned using a Karl Suss MJB-3 mask aligner. A thin (<15 nm) chromium adhesion layer and a thicker (100 nm) gold layer were deposited *via* e-beam evaporation. The remaining photo-resist was removed *via* acetone in a standard lift-off process resulting in a gold-patterned silicon surface. The patterned substrates were then soaked in a solution of ethanol and alkanethiol and rinsed.

Characterization

X-Ray diffraction patterns (XRD) of mesoporous thin films were recorded on a Scintag Pad V diffractometer using Ni-filtered $\text{CuK}\alpha$ radiation with $\lambda = 1.5418\text{\AA}$ in θ – 2θ scan mode. The morphology of the thin films after removal of the surfactant was studied by using a Hitachi S-5200 electron microscope operating at an acceleration voltage of 2.0 kV; TEM was performed on a JEOL 2010 with 200 kV acceleration voltage, equipped with a Gatan slow scan CCD camera. The sample was prepared using standard cross-section techniques, or by scratching the films on silicon substrates using tweezers. A surface acoustic wave (SAW) technique was used to characterize nitrogen sorption isotherms of mesoporous thin film samples. The samples of thin film for SAW measurement were deposited onto ST-cut quartz SAW substrates followed by calcination as described above. The SAW devices (97 MHz) on ST-quartz with Ti-primed Au transducers were designed and fabricated at Sandia National Laboratories. In a typical acoustic wave device, an alternating voltage applied to an interdigital transducer on a piezoelectric substrate generates an alternating strain, which launches an acoustic wave. An ASAP 2010 instrument was combined with the SAW device to control the relative pressure; the SAW device was used to determine the frequency. Mass change was monitored ($\sim 80 \text{ pg cm}^{-2}$ sensitivity) as a function of relative pressure, assuming that the SAW frequency is only perturbed by a mass loading variation. Surface area was estimated by using the Brunauer–Emmet–Teller (BET) equation; and the pore size was calculated by

modeling the pores as cylinders: the hydraulic radius $r = 2V/S$, where V is the pore volume and S is the surface area.

Results and discussion

Here we extend the convective assembly process to synthesize mesoporous silica films by replacing the colloidal suspension with a homogeneous alcohol solution containing surfactants, oligomeric silicate, water and hydrochloric acid. As shown in Scheme 1, the bulk of the droplet is held by the capillarity in the wedge between two substrates, forming a meniscus. While the solvent evaporates, the solution from the bulk droplet spreads to the drying region, enriching the surfactant/silica concentration at the edge of the meniscus by the convective flux of solvent. The continuous evaporation, spreading, and enriching induce surfactant and silica self-assembly from free surfactants in the bulk droplet to an ordered surfactant/silica liquid crystal mesophase in the drying region. The self-assembly process is rapid, taking ~ 5 min. The process used in this paper has the same driving force as the dip-coating process which is widely used in sol-gel science:^{6,18} both rely on the evaporation of the solvent to induce the formation of the mesophase. First, a horizontal micro-trough during the evaporation induced self-assembly process addresses shortcomings of the dip-coating technique by dramatically reducing the sample volume. Horizontal film formation from a meniscus is independent of the force of gravity and the governing equation of the process is consequently simplified, thus resulting in more straightforward design implementation.¹⁵ Secondly, this system is operated in a lower velocity range from $1\text{--}230 \mu\text{m s}^{-1}$, which is about one or two orders of magnitude lower than the dragging speed in the dip-coating process. Moreover, this technique does not require high shearing as in the spin-coating process. According to eqn (1), the film thickness is inversely proportional to the coating velocity. Combining convective self-assembly with surfactant/silica sol-gel mesophase formation allows the film thickness to be decreased from $300\text{--}500$ nm (the lowest thickness attained by dip coating)⁶ to less than 100 nm. Because the initial critical surfactant concentration, c_0 , may vary in accordance with the viscosity of the fluid, the experimental conditions under which the mesophase is being formed may differ from those reported for the dip-coating process.

Scheme 1 illustrates the scheme for direct deposition of silica/surfactant mesostructured thin films on solid substrates ((100) orientation silicon wafer) through convective self-assembly. An aliquot of $5\text{--}10 \mu\text{l}$ surfactant-silica sol solution was injected/placed at the junction of two solid surfaces (upper surface: microscopy slide, bottom surface: silicon wafer) with an angle of $23 \pm 1^\circ$. The surfactant-silica sol was entrapped there by capillarity. The electric linear motor pushes the moving/coating plate (droplet plate) and drags the liquid meniscus solution horizontally along the silicon wafer at a controlled, constant rate, v_w , ranging from 80 to $230 \mu\text{m s}^{-1}$. It is experimentally determined that the angle between the two substrates should have a range of about 15° to 40° according to the size of the instrument. To successfully implement the convective assembly method using this experiment set-up, a concave meniscus between two substrates is a must. The

reason is that the capillarity is the main force holding the meniscus initially and while coating. Therefore the angle should be large enough for sufficient volume of solution in the meniscus. On the other hand, the angle should not be larger than 40° , due to directional restriction of the electric motor that provides the linear dragging force to the meniscus. So far, there is no theoretical calculation for this angle, it is anticipated that when the process set-up is scaled up, the angle range will be different, and may have a larger range. Coatings were deposited inside a closed chamber at ambient conditions and controlled humidity ($\sim 30\%$). As the solvent evaporated, an ordered surfactant/silica mesostructured thin film was formed on the silicon wafer. Surfactants were removed *via* calcination at 450°C in air. The film thickness was measured by ellipsometry. Fig. 1 shows the thickness of calcined mesoporous thin films prepared with varying coating velocities. We can see that within the velocity range of $80\text{--}230 \mu\text{m s}^{-1}$, the film thickness is below 100 nm. Fig. 1 also demonstrates the inverse relationship between film thickness and coating velocity, which is consistent with eqn (1). On the other hand, the correlation between velocity and film thickness given in Fig. 1 also indicates the conditions where $v_c = v_w$ is satisfied. In other words, when the coating speed equals the velocity on this linear line, complete and uniform mesoporous silica thin films are formed, as proved by TEM images and X-ray diffraction (XRD) results discussed later. The concentration of the coating solution is another experimental variable that could be used to control film thickness; however, in this work the concentration of surfactant-silica sol solution was not varied.

The mesostructured silica films were synthesized primarily using the nonionic surfactant Brij-56 as the template. Fig. 2A displays representative XRD results for both the as-deposited and calcined mesoporous thin films prepared with a coating velocity of $144 \mu\text{m s}^{-1}$. For the as-deposited film, two peaks are shown in the low angle range with d -spacings of 46 \AA and 24 \AA , which can be indexed as (100) and (200) of a one-dimensional hexagonal mesostructure with lattice constant $a = 5.3$ nm. After removal of surfactants by calcination, the silica mesophase transforms to a cubic mesostructure. Owing to the one-dimensional shrinkage (vertical to the substrate) caused by

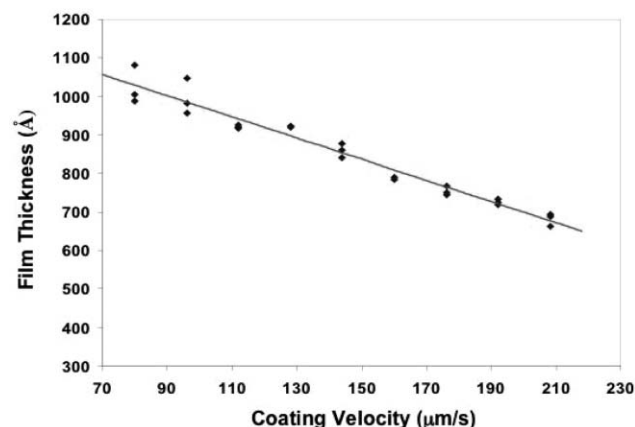


Fig. 1 Plot of mesoporous film thickness vs. coating velocity. The film was prepared by using $4 \text{ wt}\%$ Brij-56 surfactant.

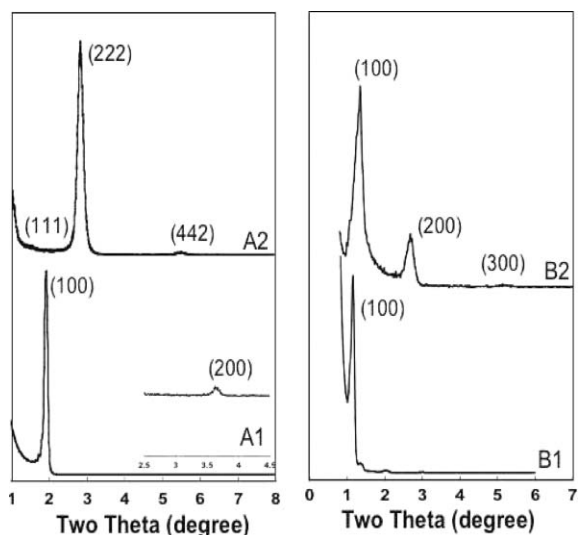


Fig. 2 Representative X-ray diffraction patterns of thin films before and after calcination. A1 was prepared using 4 wt% Brij-56 surfactant. A2 is sample A1 after calcination. B1 was prepared using 5 wt% P123. B2 is sample B1 after calcination.

calcination,¹⁹ the resulting mesoporous silica film exhibits distorted features. The XRD reflections are positioned at 60.8 Å, 31.4 Å, and 16.0 Å, and can be indexed as (111), (222), and (442) of a face-centered-cubic mesostructure with unit cell constant $a = \sim 10.5$ nm.¹⁹ In addition to Brij-56, block copolymer P123 was used to synthesize larger pore size silica films. Fig. 2B shows the XRD results of films prepared by using P123 with a coating velocity of $144 \mu\text{m s}^{-1}$. The uncalcined sample shows three reflections in the low angle range. They can be indexed as (100), (200), and (300) of a 1-D hexagonal mesostructure. After calcination, the three peaks were observed to shift to lower d -spacing range due to the shrinkage caused by calcination. Based on 1-D hexagonal symmetry, the calculated unit cell $a = \sim 7.5$ nm.

Fig. 3 shows the representative transmission electron microscopy (TEM) micrographs of a calcined film prepared using Brij-56 surfactant. The [100] plan-view TEM image (Fig. 3A) suggests unit cell parameter $a = \sim 10.6$ nm, which is consistent with the XRD results. The cross-sectional view TEM image in Fig. 3B revealed that the film exhibited substantial order throughout its thickness. The electron diffraction pattern confirmed the 3D mesostructure. The film thickness is ~ 70 nm, which is consistent with the ellipsometry results. The film is continuous and homogeneous through the whole film thickness. Fig. 3C and D show the TEM images of a mesoporous silica thin film with 1-D hexagonal mesostructure. The swirling “finger print” pattern in the plan-view TEM image (Fig. 3C) is characteristic of 1-D hexagonal mesostructure.^{4,5} The cross-sectional view image (Fig. 3D) shows different orientations of hexagonal cylindrical pore channels and [100] hexagonal arrays that are parallel to the substrate surface.

Another feature of the convective self-assembly process is the ability to deposit patterned mesoporous silica films that are essential for sensor applications. The silica–surfactant solution was spread over substrates with pre-patterned hydrophobic and hydrophilic regions created by selective growth of

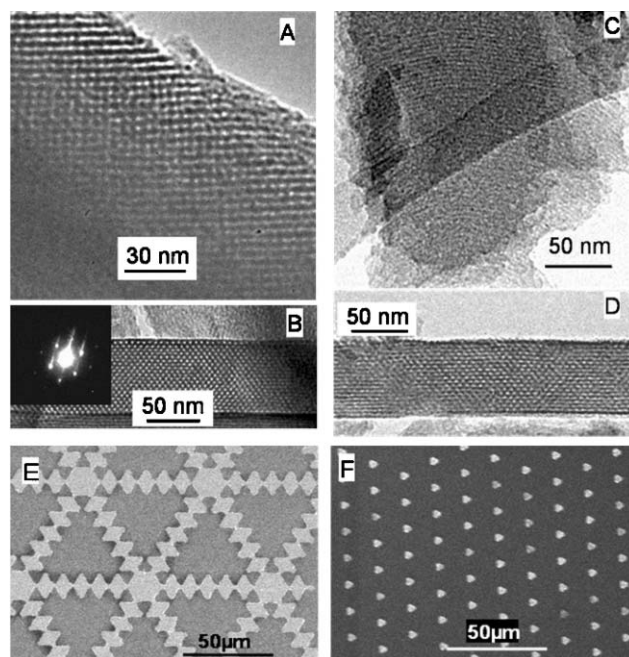


Fig. 3 Representative transmission electron microscopy images of mesoporous silica films. A: A plan-view image of the [100] orientation of a cubic-structured film prepared using 4 wt% Brij-56 surfactant. B: The cross-sectional image of the same film as in A. The inset shows the electron diffraction pattern in B. C: A plan-view image of a 1-D hexagonal film, showing swirling patterns. The film was prepared using 4 wt% Brij-56 surfactant. D: The cross-sectional image of the same film as in C, showing the [100] and [110] orientations of 1-D hexagonal mesostructure. E and F: Patterned mesoporous silica films with different feature sizes, prepared by using 4 wt% Brij-56 surfactant on pre-patterned hydrophilic–hydrophobic surfaces.

alkanethiols.⁷ The continuous evaporation, spreading, and enriching result in the formation of hydrophilic surfactant/silica mesostructured films. Through selective de-wetting of the hydrophobic regions, the final silica mesostructured films were formed exclusively on the hydrophilic patterns. In this fashion, multiple lines, arrays of dots, or other arbitrary shapes can be printed in minutes. Fig. 3E and F show SEM images that demonstrate the corresponding patterned features including isolated triangles and connected lines, circles, and triangles of different dimensions. The XRD results confirmed the mesostructures of these patterned films.

Accessibility of surfactant templated thin films is very important in order to use such films as catalysts and separation membranes, or sensors. A surface acoustic wave technique (SAW) was used to determine the physico-chemical properties of the supported thin films.²⁰ The SAW nitrogen sorption isotherms for a cubic film templated by Brij-56 are shown in Fig. 4. This illustration is a typical type IV isotherm and shows a well-defined adsorption/desorption curve between partial pressures, P/P_0 , of 0.2–0.4, indicative of a mesoporous system. The measured BET surface area is about $970 \text{ m}^2 \text{ g}^{-1}$ and the calculated pore size is 22 Å, demonstrating the accessibility of the mesoporous pore channel system. These results are similar to those of bulk powders synthesized using the same surfactant.²¹ The lack of hysteresis and absence of adsorption

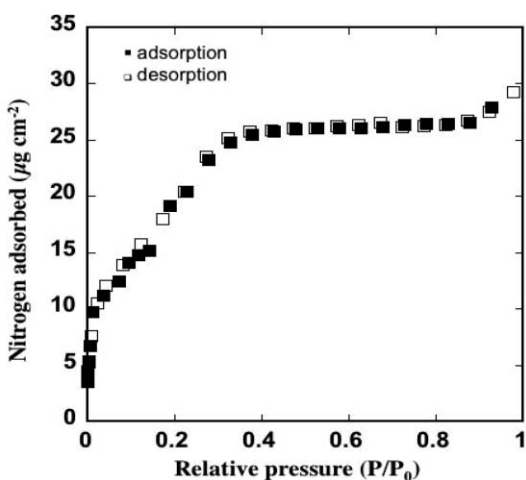


Fig. 4 Nitrogen sorption isotherms measured by using a surface acoustic wave technique. The film was prepared by using 4 wt% Brij-56 surfactant.

above a partial pressure of 0.35 indicate a uni-modal pore size distribution and the absence of interparticle meso- or macro-porosity.

Conclusion

In conclusion, we have successfully deposited mesoporous silica films with thickness less than 100 nm through combining convective self-assembly and surfactant/silica self-assembly. The supported ultra-thin film contains interconnected mesopore channels with high surface areas that could be used in applications in molecular separation, catalysis and sensors. Owing to the ultra-thin film thickness, the mesoporous film will have fast transport, enabling quick response in sensor applications. The combined self-assembly process relies on the evaporation of the solvents to form ordered nanostructures. Thus, it is practical to deposit multifunctional hybrid films through the same process by introducing functional elements into the coating solutions, such as dye molecules,^{3,7} nanocrystals,^{22–24} and functional precursors,²⁵ etc. Furthermore, the ability to deposit patterned films ultimately makes this combined technique ideal for device fabrication.

Acknowledgements

This work was partially supported by the U.S. Department of Energy (DOE) Basic Energy Sciences Program, Sandia National Laboratory's Laboratory Directed R&D program, and Center for Integrated Nanotechnologies (CINT). TEM studies were performed in the Department of Earth and Planetary Science at the University of New Mexico. We

acknowledge the use of the SEM facility supported by the NSF EPSCOR and NNIN grants. Sandia is a multi-program laboratory operated by Sandia Corporation, a Lockheed Martin Company, for the United States Department of Energy's National Nuclear Security Administration under Contract DE-AC04-94AL85000.

References

- 1 M. E. Davis, *Nature*, 2002, **417**, 813.
- 2 H. Y. Fan, H. R. Bentley, K. R. Kathan, P. Clem, Y. F. Lu and C. J. Brinker, *J. Non-Cryst. Solids*, 2001, **285**, 79.
- 3 P. D. Yang, G. Wirsberger, H. C. Huang, S. R. Cordero, M. D. McGehee, B. Scott, T. Deng, G. M. Whitesides, B. F. Chmelka, S. K. Buratto and G. D. Stucky, *Science*, 2000, **287**, 465.
- 4 H. Yang, A. Kuperman, N. Coombs, S. Mamiche-Afara and G. Ozin, *Nature*, 1996, **379**, 703.
- 5 I. Aksay, M. Trau, S. Manne, I. Honma, N. Yao, L. Zhou, P. Fenter, P. Eisenberger and S. Gruner, *Science*, 1996, **273**, 892.
- 6 C. J. Brinker, Y. F. Lu, A. Sellinger and H. Y. Fan, *Adv. Mater.*, 1999, **11**, 579.
- 7 H. Y. Fan, Y. F. Lu, A. Stump, S. T. Reed, T. Baer, R. Schunk, V. PerezLuna, G. P. Lopez and C. J. Brinker, *Nature*, 2000, **405**, 56.
- 8 Y. F. Lu, H. Y. Fan, A. Stump, T. L. Ward, T. Rieker and C. J. Brinker, *Nature*, 1999, **398**, 223.
- 9 N. Nishiyama, S. Tanaka, Y. Egashira, Y. Oku and K. Ueyama, *Chem. Mater.*, 2003, **15**, 1006.
- 10 S. Tanaka, N. Nishiyama, Y. Oku, Y. Egashira and K. Ueyama, *J. Am. Chem. Soc.*, 2004, **126**, 4854.
- 11 S. Tanaka, H. Tada, T. Maruo, N. Nishiyama, Y. Egashira and K. Ueyama, *Thin Solid Films*, 2006, **495**, 186.
- 12 C. Kresge, M. Leonowicz, W. Roth, C. Vartuli and J. Beck, *Nature*, 1992, **359**, 710.
- 13 N. D. Denkov, O. D. Velev, P. A. Kralchevsky, I. B. Ivanov, H. Yoshimura and K. Nagayama, *Langmuir*, 1992, **8**, 3183.
- 14 N. D. Denkov, O. D. Velev, P. A. Kralchevsky, I. B. Ivanov, H. Yoshimura and K. Nagayama, *Nature*, 1993, **361**, 26.
- 15 B. G. Prevo and O. D. Velev, *Langmuir*, 2004, **20**, 2099.
- 16 K. Nagayama, *Phase Transitions*, 1993, **45**, 185.
- 17 A. S. Dimitrov and K. Nagayama, *Langmuir*, 1996, **12**, 1303.
- 18 C. J. Brinker and G. W. Scherer, *Sol-gel science: the physics and chemistry of sol-gel processing*, Academic Press Inc, San Diego, CA, 1990.
- 19 D. A. Doshi, N. K. Huesing, M. C. Lu, H. Y. Fan, Y. F. Lu, K. Simmons, B. G. Potter, A. J. Hurd and C. J. Brinker, *Science*, 2000, **290**, 107.
- 20 G. C. Frye, S. J. Martin, A. J. Ricco and C. J. Brinker, *ACS Symp. Ser.*, 1989, **403**, 208.
- 21 D. Y. Zhao, Q. S. Huo, J. L. Feng, B. F. Chmelka and G. D. Stucky, *J. Am. Chem. Soc.*, 1998, **120**, 6024.
- 22 H. Fan, A. Wright, J. Gabaldon, A. Rodriguez, C. Brinker and Y. Jiang, *Adv. Funct. Mater.*, 2006, **16**, 891.
- 23 H. Y. Fan, E. W. Leve, C. Scullin, J. Gabaldon, D. Tallant, S. Bunge, T. Boyle, M. C. Wilson and C. J. Brinker, *Nano Lett.*, 2005, **5**, 645.
- 24 H. Y. Fan, K. Yang, D. Boye, T. Sigmon, K. Malloy, H. Xu, G. P. Lopez and C. Brinker, *Science*, 2004, **304**, 567.
- 25 Y. F. Lu, Y. Yang, A. Sellinger, M. C. Lu, J. M. Huang, H. Y. Fan, R. Haddad, G. Lopez, A. R. Burns, D. Y. Sasaki, J. Shelnett and C. J. Brinker, *Nature*, 2001, **410**, 913.